REPORTS OF PRACTICAL ONCOLOGY AND RADIOTHERAPY 22 (2017) 290–294

Available online at www.sciencedirect.com

ScienceDirect

journal homepage: http://www.elsevier.com/locate/rpor

Original research article

Effect of tumor amplitude and frequency on 4D modeling of Vero4DRT system

Hideharu Miura[a,*], Shuichi Ozawa[a,b], Masahiro Hayata[a], Shintaro Tsuda[a], Kiyoshi Yamada[a], Yasushi Nagata[a,b]

[a] Hiroshima High-Precision Radiotherapy Cancer Center, Japan
[b] Department of Radiation Oncology, Institute of Biomedical & Health Science, Hiroshima University, Japan

ARTICLE INFO

Article history:
Received 11 May 2016
Received in revised form
7 October 2016
Accepted 27 February 2017
Available online 5 May 2017

Keywords:
Correlation model
Predictive uncertainty
IR tracking
Respiratory surrogates
Vero4DRT

ABSTRACT

Background: An important issue in indirect dynamic tumor tracking with the Vero4DRT system is the accuracy of the model predictions of the internal target position based on surrogate infrared (IR) marker measurement. We investigated the predictive uncertainty of 4D modeling using an external IR marker, focusing on the effect of the target and surrogate amplitudes and periods.

Methods: A programmable respiratory motion table was used to simulate breathing induced organ motion. Sinusoidal motion sequences were produced by a dynamic phantom with different amplitudes and periods. To investigate the 4D modeling error, the following amplitudes (peak-to-peak: 10–40 mm) and periods (2–8 s) were considered. The 95th percentile 4D modeling error (4D-$E_{95\%}$) between the detected and predicted target position ($\mu + 2\mathrm{SD}$) was calculated to investigate the 4D modeling error.

Results: 4D-$E_{95\%}$ was linearly related to the target motion amplitude with a coefficient of determination $R^2 = 0.99$ and ranged from 0.21 to 0.88 mm. The 4D modeling error ranged from 1.49 to 0.14 mm and gradually decreased with increasing target motion period.

Conclusions: We analyzed the predictive error in 4D modeling and the error due to the amplitude and period of target. 4D modeling error substantially increased with increasing amplitude and decreasing period of the target motion.

1. Introduction

Breathing-induced organ motion is one of the issues causing uncertainties during beam delivery. Several studies have reported that breathing produces the greatest movement in the caudal–cranial (CC) direction close to the diaphragm, such as tumors in the lower lung lobes, and upper abdominal tumors, such as liver or pancreas tumors.[1] To compensate for breathing-induced organ motion, an internal margin should be added around the clinical target volume (CTV) to account for respiratory tumor motion.[2] The planning target volume (PTV) adds margins around the CTV. However, this margin results in an increased dose to the normal

---

[*] *Corresponding author at*: Hiroshima High-Precision Radiotherapy Cancer Center, 3-2-2, Futabanosato, Higashiku-ku, Hiroshima 732-0057, Japan.

E-mail address: miura@hiprac.jp (H. Miura).

http://dx.doi.org/10.1016/j.rpor.2017.02.012

tissue, which increases the risk of normal tissue toxicity and limits dose escalation and, in turn, leads to a higher probability of radiation damage.[3] Breathing-induced organ motion-compensated treatment techniques include delivery techniques such as motion-encompassing methods, breath holding,[4] forced shallow breathing,[5] and respiratory gating.[6] Advanced motion-compensated treatment techniques are based on modeling the respiratory motion.[7]

The Vero4DRT system (MHI-TM2000, Mitsubishi Heavy Industries, Ltd., Japan, and BrainLAB, Feldkirchen, Germany) is equipped with infrared (IR) marker based indirect dynamic tumor tracking (DTT), which is a fairly recent breathing-induced organ motion compensation technique. External IR markers are placed either on the chest or on the abdomen to create 4D modeling between external and internal motion. An important issue in indirect DTT of the Vero4DRT system is accuracy of the model prediction of the internal target position based on the surrogate IR marker measurements. The purpose of this study was to investigate the uncertainty in 4D modeling using the external IR markers, with a focus on the effect of target and surrogate amplitudes and periods.

2. Materials and methods

2.1. *Vero4DRT system*

The Vero4DRT system is described elsewhere.[12,13] Briefly, it features a gimbaled X-ray head mounted on an O-ring gantry with a C-band klystron, a system-specific fixed jaw, and a multileaf collimator. The gimbaled X-ray head can swing along two orthogonal axes up to ±2.5° (swings the beam up to ±41.9 mm in each direction on the isocenter plane), allowing pan and tilt motion of the linac. The nominal maximum speed of the pan and tilt rotations is 9 °/s. The rotation accuracy of the gimbaled X-ray head is within ±0.1 mm.[10] The Vero4DRT system uses a fully integrated target positioning concept, an ExacTrac system version 3.5.3 (BrainLAB AG, Feldkirchen, Germany) automated IR camera mounted on the ceiling of the treatment room, and two orthogonal kV X-ray imaging systems attached to the O-ring at 45° from the MV beam axis. The kV X-ray imaging systems acquire cone-beam computed tomography data using the O-ring rotation. Hence, Vero4DRT is clinically capable of IR-based indirect DTT for respiratory-induced tumor motion, as in the lung, liver, and pancreas. The Vero4DRT system continuously monitors the position of the IR markers on the patient's abdominal wall using the IR camera of the ExacTrac system. The positions of IR markers on the abdominal wall are also used to predict the future target position based on 4D modeling.

2.2. *Experimental*

Fig. 1 shows the entire phantom system. A programmable respiratory motion table (CIRS Inc., Norfolk, VA) was used to simulate a breathing induced organ motion. The motion table consists of two tables, the first moves in the horizontal direction and the second in the vertical direction. The motion of the two tables is synchronized. A cube phantom containing a metal ball 1.0 cm in diameter is embedded in its center. At least two fiducial markers are required for establishing the 4D-modeling. Two small iron markers (2.0 mm in diameter) as fiducial markers were attached to the cube phantom surface. The cube phantom was taken using a computed tomography (CT) (Optima CT 580 W; GE Healthcare, Milwaukee, WI). The iPlan RT Dose™ treatment planning system version 4.5.3 (BrainLAB, Feldkirchen, Germany) was used for plan design. The metal ball was contoured as a target. A single photon beam was set at a gantry angle of 0°. The center of the cube phantom was set up at the isocenter on the horizontal direction motion table. The IR marker phantom, as the surrogate signal, was positioned on the vertical direction motion table. Sinusoidal motion sequences were produced by the dynamic phantom with different amplitudes and periods. To investigate the 4D modeling error, the following amplitudes and frequencies were used.

(1) Target motion dependence: the amplitude of the target motion ranged from 10 to 40 mm, the period was fixed at 4 s, and the IR marker motion amplitude was fixed at 10 mm.
(2) Target motion period dependence: the period of the target motion ranged between 2 and 8 s, the target amplitude was fixed at 20 mm, and the IR marker motion amplitude was fixed at 10 mm.
(3) IR marker motion dependence: the amplitude of the IR marker ranged from 5 to 30 mm, the period was fixed at 4 s, and the target motion amplitude was set at 10, 20, 30, and 40 mm to investigate the correlation between the target and IR motions.

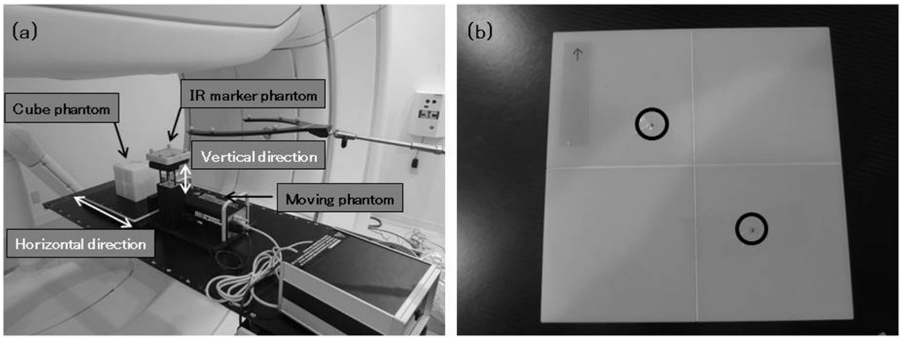

Fig. 1 – (a) The cube phantom and (b) the two steel markers (black circles) attached on the cube phantom.

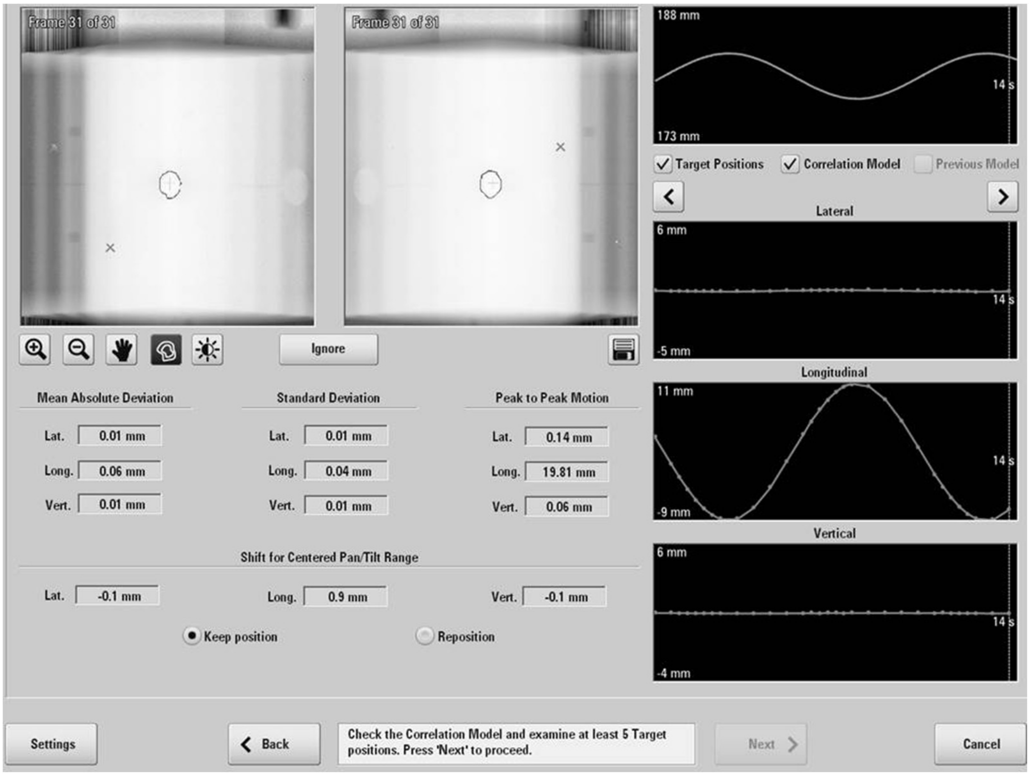

☑ Target Positions ☑ Correlation Model ☐ Previous Model

	Mean Absolute Deviation	Standard Deviation	Peak to Peak Motion
Lat.	0.01 mm	0.01 mm	0.14 mm
Long.	0.06 mm	0.04 mm	19.81 mm
Vert.	0.01 mm	0.01 mm	0.06 mm

Shift for Centered Pan/Tilt Range

Lat. -0.1 mm Long. 0.9 mm Vert. -0.1 mm

● Keep position ○ Reposition

Check the Correlation Model and examine at least 5 Target positions. Press 'Next' to proceed.

Fig. 2 – Screen capture of 4D modeling result.

A motion table was only moved in the CC direction. We did not use irradiation in this study.

2.3. 4D modeling

4D modeling with the Vero4DRT system is described elsewhere.[8–14] Briefly, the two iron markers on the cube phantom and the IR markers on the vertical table are simultaneously acquired to calculate the 4D modeling function. A pair of orthogonal kV X-rays at gantry angles of 315° and 45° acquired the positions of the iron markers every 320 or 640 ms. The sampling interval of the kV X-ray images automatically changed to 640 ms when the velocity of the IR marker motion decreased. The X-ray parameters were 110 kV, 100 mA, and 5 ms. The acquisition times ranged from 20 to 40 s. The centroid of the two iron markers during motion is defined as the detected target position. The motion of the surrogate was acquired from the IR markers attached on the cube phantom monitored by the IR camera on the ceiling of the treatment room every 16.7 ms. The 4D modeling function was a quadratic function of the IR marker position (P_{IR}) and velocity,

$$P_{predict} = aP_{IR}{}^2 + bP_{IR} + c + dv_{IR}{}^2 + ev_{IR}, \qquad (1)$$

where $P_{predict}$ is the predicted target position and v_{IR} is the vertical velocity of the IR markers. Parameters a, b, c, d, and e were optimized by minimizing the residual errors between $P_{predict}$ and the detected target position for each IR marker. After analyzing the 4D motion data of the target and IR marker motions, the 4D modeling function was calculated by the ExacTrac system. Absolute mean (μ) difference value and standard deviation (SD) between predicted and detected target positions was displayed on the screen of the Vero4DRTsystem in the 4D-modeling phase (Fig. 2).

2.4. Data analysis

The 4D modeling function error was calculated from the absolute difference between the detected and predicted target position in the CC direction. The μ and SD of the absolute 4D modeling function error were analyzed, and the 95th percentile 4D modeling error (4D-$E_{95\%}$) between the detected and predicted target position (μ + 2SD) was calculated.

3. Results

Fig. 3 shows the predicted and detected target motion in 4D modeling, and the differences for the (a) 10 and (b) 40 mm target motion amplitudes, respectively. The 4D modeling error is maximum at the begin- and end-inspiration phases.

Fig. 4 shows 4D-$E_{95\%}$ as a function of the target motion amplitude. The 4D modeling error gradually increased with increasing target motion amplitude. 4D-$E_{95\%}$ was linearly related to target motion with a coefficient of determination $R^2 = 0.99$ and ranged from 0.21 to 0.88 mm.

Fig. 5 shows 4D-$E_{95\%}$ as a function of the target motion period. The 4D modeling error gradually decreased with

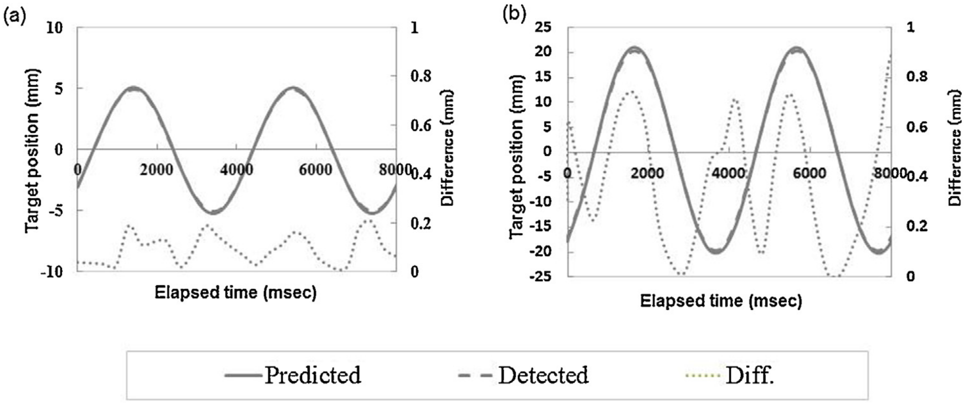

Fig. 3 – Predicted and detected target motion for the peak-to-peak motion amplitudes of (a) 10 and (b) 40 mm with a breathing period of 4 s.

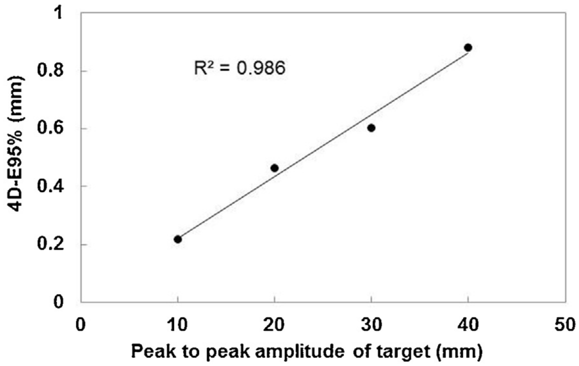

Fig. 4 – 4D-$E_{95\%}$ as a function of the peak-to-peak target amplitude. The 4D modeling error increased with increasing target motion amplitude.

increasing target motion period and ranged from 1.49 to 0.14 mm.

Fig. 6 shows 4D-$E_{95\%}$ as a function of the surrogate IR marker motion amplitude. The 4D modeling error does not depend on the IR marker motion amplitude.

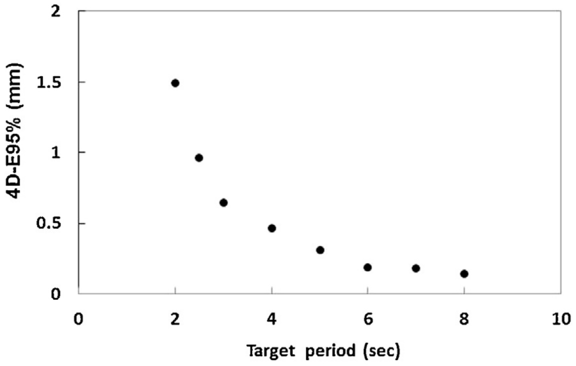

Fig. 5 – 4D-$E_{95\%}$ as a function of the target motion period. The 4D modeling error decreased with increasing target motion period.

4. Discussion and conclusion

We investigated the effect of target and IR surrogate signals in the 4D modeling process in DTT. The phantom study suggested that the 4D modeling error strongly depended on the target motion amplitude and period. The 4D modeling error increased with increasing target motion amplitude and peak position and sometimes overestimated the predicted position. Indirect DTT systems rely on external surrogate signals attached to the patient to predict the target position. Establishing 4D modeling is needed to encourage patients to breathe periodically and at a higher period.

A limitation of this study was that it was performed under 1D sinusoidal regulated moving target in the CC direction only. Further studies should examine the effect of 4D modeling error under various condition breathing patterns. Miura et al. reported that a non-regular breathing pattern such a volunteer was measured using a chamber and film, and 4D-modeling error (4D-$E_{95\%}$) was 0.34 mm.[16] In clinical situation, patient breathing is changed in patterns due to anxiety, Chronic Obstructive Pulmonary Disease (COPD), coughing, sighing and

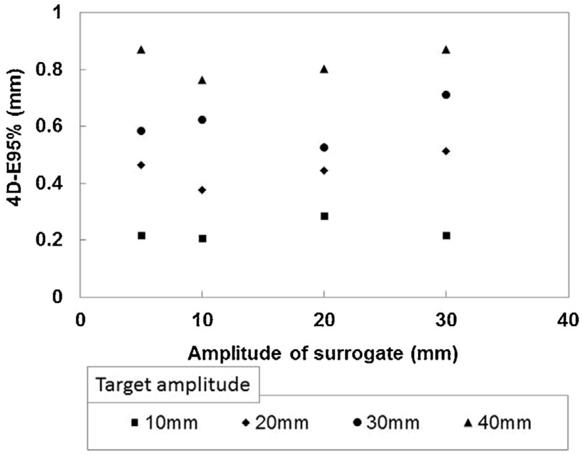

Fig. 6 – 4D-$E_{95\%}$ as a function of the IR marker motion. The 4D modeling error does not depend on the IR marker motion amplitude.

other random events. As for clinical data, Ebe et al. reported that absolute mean difference +2SD was 0.20–0.85 mm using a 1D moving phantom and 16 trajectories in six patients.[17] This study was the only investigation of the 4D-modeling error. Future investigations of the 4D modeling error should concentrate on the tracking accuracy. A good correlation is found between the 4D modeling error and a light field measurement results ($R^2 = 0.998$).[18] Target position is calculated from the displacements of the IR markers using the 4D model during beam delivery, and gimbaled X-ray head is swung. Thus, adding margins to compensate for 4D-modeling errors should be discussed with the user.

Estimating the 4D modeling error is important because decisions about the CTV–PTV margin are based on the gimbal position error. Adding margins to compensate for the 4D modeling error need to be evaluated before treatment and, in particular, for large target motion amplitude and short breathing period. It should be noted that one should be very careful in shrinking the margins. Van Herk reported that a PTV margin of 5 mm or less is highly unrealistic for most tumors.[19] Giraud et al. showed that the CTV margin must be increased to 8 and 6 mm for adenocarcinoma and squamous cell carcinoma to cover 95% of microscopic extension, respectively.[20] Pepin et al.[15] and Mukumoto et al.[11] also suggested that a dry-run treatment session prior to treatment planning is required to add patient-specific margins to cover the positional tracking error in synchronous respiratory tracking and Vero4DRT systems.

In conclusions, we analyzed the predictive error in 4D modeling as a function of the amplitude and period of the target and IR marker in the Vero4DRT system. The 4D modeling error substantially increased with increasing amplitude and decreasing period owing to target motion.

Presentation at a conference

None declared.

Clinical trial registration

None declared.

Conflict of interest

None declared.

Financial disclosure

None declared.

REFERENCES

1. Keall PJ, Mageras GS, Balter JM, et al. The management of respiratory motion in radiation oncology report of AAPM Task Group 76. *Med Phys* 2006;**33**:3874–900.
2. ICRU. *Prescribing, recording, and reporting photon beam therapy. ICRU Report Volume* 50. Bethesda: International Commission on Radiation Units and Measurements; 1993.
3. Seppenwoolde Y, Lebesque JV, De Jaeger K, et al. Comparing different NTCP models that predict the incidence of radiation pneumonitis. Normal tissue complication probability. *Int J Radiat Oncol Biol Phys* 2003;**55**:724–35.
4. Mah D, Hanley J, Rosenzweig KE, et al. Technical aspects of the deep inspiration breath hold technique in the treatment of thoracic cancer. *Int J Radiat Oncol Biol Phys* 2003;**48**: 1175–85.
5. Negoro Y, Nagata Y, Aoki T, et al. The effectiveness of an immobilization device in conformal radiotherapy for lung tumor: reduction of respiratory tumor movement and evaluation of the daily setup accuracy. *Int J Radiat Oncol Biol Phys* 2001;**50**:889–98.
6. Shirato H, Shimizu S, Kunieda T, et al. Physical aspects of a real-time tumor-tracking system for gated radiotherapy. *Int J Radiat Oncol Biol Phys* 2000;**48**:1187–95.
7. Schweikard A, Shiomi H, Adler J. Respiration tracking in radiosurgery. *Med Phys* 2004;**31**:2738–41.
8. Kamino Y, Takayama K, Kokubo M, et al. Development of a four-dimensional image-guided radiotherapy system with a gimbaled X-ray head. *Int J Radiat Oncol Biol Phys* 2006;**66**:271–8.
9. Nakamura M, Sawada A, Ishihara Y, et al. Dosimetric characterization of a multileaf collimator for a new four-dimensional Image-guided radiotherapy system with a gimbaled X-ray head, MHI-TM2000. *Med Phys* 2010;**37**:4684–91.
10. Miyabe Y, Sawada A, Takayama K, et al. Positioning accuracy of a new image-guided radiotherapy system. *Med Phys* 2011;**38**:2535–41.
11. Mukumoto N, Nakamura M, Sawada A, et al. Accuracy verification of infrared marker-based dynamic tumor-tracking irradiation using the gimbaled X-ray head of the Vero4DRT (MHI-TM2000). *Med Phys* 2013;**40**:041706.
12. Takayama K, Mizowaki T, Kokubo M, et al. Initial validations for pursuing irradiation using a gimbals tracking system. *Radiother Oncol* 2009;**93**:45–9.
13. Akimoto M, Nakamura M, Mukumoto N, et al. Predictive uncertainty in infrared marker-based dynamic tumor tracking with Vero4DRT. *Med Phys* 2013;**40**:091705.
14. Nakamura M, Akimoto M, Mukumoto N, et al. Influence of the correlation modeling period on the prediction accuracy of infrared marker-based dynamic tumor tracking using a gimbaled X-ray head. *Phys Med* 2015;**31**:204–9.
15. Pepin EW, Wu H, Zhang Y, Lord B. Correlation and prediction uncertainties in the cyberknife synchrony respiratory tracking system. *Med Phys* 2011;**38**:4036–44.
16. Miura H, Ozawa S, Tsuda S, et al. Quality assurance for dynamic tumor tracking using the Vero4DRT system. *Int J Cancer Ther Oncol* 2016;**4**:4112.
17. Ebe K, Sugimoto S, Utsunomiya S, et al. Development of a video image-based QA system for the positional accuracy of dynamic tumor tracking irradiation in the Vero4DRT system. *Med Phys* 2015;**42**(8):4745–54.
18. Miura H, Ozawa S, Hayata M, et al. Simple quality assurance method of dynamic tumor tracking with the gimbaled linac system using a light field. *J Appl Clin Med Phys* 2016; **17**(5):6376.
19. Van Herk M. Will IGRT live up to its promise? *Acta Oncol* 2008;**47**(7):1186–7.
20. Giraud P, Antoine M, Larrouy A, et al. Evaluation of microscopic tumor extension in non-small-cell lung cancer for three-dimensional conformal radiotherapy planning. *Int J Radiat Oncol Biol Phys* 2000;**48**:1015–24.